

LASER APPLICATIONS AND OTHER TOPICS IN QUANTUM ELECTRONICS

PACS numbers: 42.62.Be; 42.25.Ja; 42.25.Lc; 87.18.–h
DOI: 10.1070/QE2015v045n03ABEH015333

Mueller-matrix mapping of biological tissues in differential diagnosis of optical anisotropy mechanisms of protein networks

V.A. Ushenko, M.I. Sidor, Yu.F. Marchuk, N.V. Pashkovskaya, D.R. Andreichuk

Abstract. **We report a model of Mueller-matrix description of optical anisotropy of protein networks in biological tissues with allowance for the linear birefringence and dichroism. The model is used to construct the reconstruction algorithms of coordinate distributions of phase shifts and the linear dichroism coefficient. In the statistical analysis of such distributions, we have found the objective criteria of differentiation between benign and malignant tissues of the female reproductive system. From the standpoint of evidence-based medicine, we have determined the operating characteristics (sensitivity, specificity and accuracy) of the Mueller-matrix reconstruction method of optical anisotropy parameters and demonstrated its effectiveness in the differentiation of benign and malignant tumours.**

Keywords: *Mueller matrix, linear birefringence, linear dichroism, polarisation, statistical moments, diagnostics.*

1. Introduction

Biological tissues represent structurally inhomogeneous optically anisotropic absorbing media. To describe the interaction of polarised light with such complex systems requires more general approximations based on the use of the Mueller-matrix formalism, which is widely employed in many practical techniques of biological and medical research [1–12]. One of the independent directions of matrix optics is laser polarimetry of histological sections of biological tissues [13]. It allows one to establish the relationship between a set of statistical moments of the 1st-to-4th orders [14–19], which characterise the distribution of Mueller-matrix elements, and the linear birefringence parameters of fibrillar protein networks in human biological tissues. This technique has enabled us to diagnose oncologic changes of skin derma, epithelial and connective tissue of the female reproductive system, etc. [20–22]. At the same time, the problem of the 'precancer–cancer' state differentiation still remains unsolved. However, optical anisotropy of biological tissues is associated not only with linear birefringence, but also with other effects. Therefore, for the further development of Mueller-matrix mapping functionality, important is the creation of relevant techniques that take into account the influence of other mechanisms (e.g., linear dichroism of protein networks).

The aim of this work is to provide a method of Mueller-matrix reconstruction of the parameters characterising linear birefringence and dichroism of biological tissues in order to differentiate benign and malignant tumours of the uterine wall.

V.A. Ushenko, M.I. Sidor Yuriy Fedkovych Chernivtsi National University, ul. Kotsyubinskogo 2, 58012 Chernivtsi, Ukraine; e-mail: yuriyu@gmail.com;
Yu.F. Marchuk, N.V. Pashkovskaya, D.R. Andreichuk Bukovinian State Medical University, Teatral'naya pl. 3, 58000 Chernivtsi, Ukraine

Received 28 October 2013; revision received 14 February 2014
Kvantovaya Elektronika **45** (3) 265–269 (2015)
Translated by I.A. Ulitkin

2. Brief description of the method theory

The Mueller-matrix description of the optical anisotropy mechanisms of biological tissues is based on the following model representations:

1. Fibrillar protein (collagen, elastinic, myosin) networks exhibit linear birefringence and linear dichroism [10].

2. Optical manifestations of these mechanisms are exhaustively fully described by matrix operators of linear birefringence

$$\{D\} = \begin{Vmatrix} 1 & 0 & 0 & 0 \\ 0 & d_{22} & d_{23} & d_{24} \\ 0 & d_{32} & d_{33} & d_{34} \\ 0 & d_{42} & d_{43} & d_{44} \end{Vmatrix}, \tag{1}$$

$$d_{ik} = \begin{cases} d_{22} = \cos^2 2\rho + \sin^2 2\rho \cos\delta, \\ d_{23} = d_{32} = \cos 2\rho \sin 2\rho (1 - \cos\delta), \\ d_{33} = \sin^2 2\rho + \cos^2 2\rho \cos\delta, \\ d_{24} = -d_{42} = \sin 2\rho \sin\delta, \\ d_{34} = -d_{43} = \cos 2\rho \sin\delta, \\ d_{44} = \cos\delta \end{cases}$$

(ρ is orientation of the optical axis of the fibril and δ is the phase shift between orthogonal linearly polarised components of the light beam amplitude) and linear dichroism

$$\{\Psi\} = \begin{Vmatrix} 1 & \varphi_{12} & \varphi_{13} & 0 \\ \varphi_{21} & \varphi_{22} & \varphi_{23} & 0 \\ \varphi_{31} & \varphi_{32} & \varphi_{33} & 0 \\ 0 & 0 & 0 & \varphi_{44} \end{Vmatrix}, \tag{2}$$

$$\varphi_{ik} = \begin{cases} \varphi_{12} = \varphi_{21} = (1 - \Delta\tau)\cos 2\rho, \\ \varphi_{13} = \varphi_{31} = (1 - \Delta\tau)\sin 2\rho, \\ \varphi_{22} = (1 + \Delta\tau)\cos^2 2\rho + 2\sqrt{\Delta\tau}\sin^2 2\rho, \\ \varphi_{23} = \varphi_{32} = (1 - \Delta\tau)\sin 2\rho, \\ \varphi_{33} = (1 + \Delta\tau)\sin^2 2\rho + 2\sqrt{\Delta\tau}\cos^2 2\rho, \\ \varphi_{44} = 2\sqrt{\Delta\tau} \end{cases}$$

($\Delta\tau = \tau_x/\tau_y$; $\tau_x = \tau\cos\rho$, $\tau_y = \tau\sin\rho$ are the absorption coefficients of orthogonal linearly polarised components of the light beam amplitude).

The resulting Mueller matrix of an optically anisotropic network can be written in the form:

$$\{M\} = \{D\}\{\Psi\}$$

$$= \begin{Vmatrix} 1 & \varphi_{12} & \varphi_{13} & 0 \\ (d_{22}\varphi_{21}+d_{32}\varphi_{31}) & (d_{22}\varphi_{22}+d_{32}\varphi_{32}) & (d_{22}\varphi_{23}+d_{32}\varphi_{33}) & d_{24}\varphi_{44} \\ (d_{32}\varphi_{21}+d_{33}\varphi_{31}) & (d_{32}\varphi_{22}+d_{33}\varphi_{32}) & (d_{32}\varphi_{23}+d_{33}\varphi_{33}) & d_{34}\varphi_{44} \\ (d_{42}\varphi_{21}+d_{43}\varphi_{31}) & (d_{42}\varphi_{22}+d_{43}\varphi_{32}) & (d_{42}\varphi_{23}+d_{43}\varphi_{33}) & d_{44}\varphi_{44} \end{Vmatrix}$$

$$= \begin{Vmatrix} 1 & M_{12} & M_{13} & 0 \\ M_{21} & M_{22} & M_{23} & M_{24} \\ M_{31} & M_{32} & M_{33} & M_{34} \\ M_{41} & M_{42} & M_{43} & M_{44} \end{Vmatrix}. \quad (3)$$

Comparison of matrices (1)–(3) allows one to obtain invariants of the 'polarisation reconstruction' of the linear birefringence (δ) and dichroism ($\Delta\tau$) parameters of biological tissues:

$$\delta = \arccos\left[\frac{M_{44}}{2\sqrt{1-(M_{\bar{1}2}^2+M_{\bar{1}3}^2)}}\right], \quad (4)$$

$$\Delta\tau = 1-(M_{\bar{1}2}^2+M_{\bar{1}3}^2). \quad (5)$$

Thus, by measuring the coordinate distributions of the matrix elements with the dimension $m\times n$ (the number of digital camera pixels of the Stokes polarimeter [13])

$$M_{ik} \equiv \begin{cases} M_{44}, \\ M_{12}, \\ M_{13} \end{cases}$$

we can determine the maps of the optical anisotropy parameters δ and $\Delta\tau$ (having the same dimensions) of protein networks of biological tissues.

3. Objects of research, methodology and processing algorithms

As objects of research we used optically thin (geometric thickness, $d \approx 30$ μm; attenuation coefficient, $\tau < 0.1$) histological sections of biopsies of benign (fibroids – group 1) and malignant (adenocarcinoma – group 2) tumours of the uterus.

Histological sections were prepared by standard methods on a freezing microtome. Each of these layers is characterised by the presence of optically anisotropic protein networks. Birefringence and dichroism of the uterine wall, formed by connective and muscular tissue, are caused by collagen and myosin fibres [14–19].

Coordinate distributions M_{ik} were measured using a standard Stokes polarimeter (Fig. 1) [13].

The sample (*6*) was illuminated by a collimated ($\varnothing = 2\times10^3$ μm) beam from a low-power He–Ne laser ($W = 5$ mW, $\lambda = 0.6328$ μm). The polarising illuminator consisted of quarter-wave plates (*3*, *5*) and polariser (*4*). The histological section in question (*6*) was sequentially probed with a laser beam having linear (azimuth angles of 0°, 90°, +45°) and right-hand circular ($\otimes$) polarisations. The images obtained using a polarising microscope objective (*7*) (Nikon CFI Achromat P, focal length of 30 mm, numerical aperture of 0.1, 4× magnification) were projected into the plane of the photosensitive

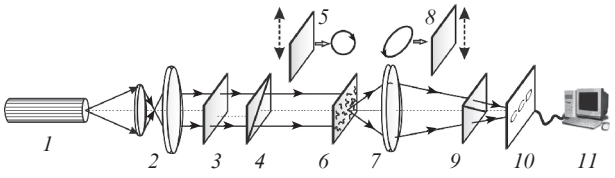

Figure 1. Optical scheme of the polarimeter (see explanations in the text): (*1*) He–Ne laser; (*2*) collimator (spatial frequency filter); (*3*) stationary quarter-wave plate; (*4*) polariser; (*5*, *8*) mechanically movable quarter-wave plates; (*6*) object of study; (*7*) microobjective; (*9*) analyser; (*10*) CCD-camera; (*11*) personal computer.

area ($m\times n$ = 800×600 pixels) of the CCD-camera (*10*) [The Imaging Source DMK 41AU02.AS, monochrome 1/2″ CCD, Sony ICX205AL (progressive scan); the resolution of 1280×960 pixels, the photosensitive area of 7600×6200 μm, the sensitivity of 0.05 lx, the 8-bit dynamic range, the SNR of 9 bits, the deviation from the linear photosensitive of no more than 15%]. The images of the histological sections (*6*) were analysed using a polariser-analyser (*9*) and a quarter-wave plate (*8*). For each type of the probe beam polarisation we measured the Stokes-vector parameters $S_i^{0,45,90,\otimes}$ at all points of the digital image:

$$S_1^{0,45,90,\otimes} = I_{\otimes}^{0,45,90,\otimes} + I_{\oplus}^{0,45,90,\otimes},$$
$$S_4^{0,45,90,\otimes} = I_{\otimes}^{0,45,90,\otimes} - I_{\oplus}^{0,45,90,\otimes}. \quad (6)$$

Here, $I_{\otimes}^{0,45,90,\otimes}$, $I_{\oplus}^{0,45,90,\otimes}$ are the intensities of the right- and left-hand circularly polarised components of the filtered laser light.

Then we calculated 'information relevant' Mueller-matrix elements M_{ik} of the histological section using the relations

$$M_{12} = 0.5(S_1^0 - S_1^{90}),$$
$$M_{13} = S_1^{45} - 0.5(S_1^0 - S_1^{90}), \quad (7)$$
$$M_{44} = S_4^{\otimes} - 0.5(S_4^0 + S_1^{90}).$$

On the basis of (7) with the help of (4) and (5) we determined the maps of linear birefringence δ and linear dichroism $\Delta\tau$ of the histological section of the uterine wall tumour.

For an objective assessment of the distributions

$$q \equiv \begin{cases} M_{ik}, \\ \delta, \\ \Delta\tau \end{cases}$$

we calculated a set of statistical moments of the 1st-to-4th orders

$$Z_1 = \frac{1}{N}\sum_{j=1}^{N}|q|, \quad Z_2 = \left(\frac{1}{N}\sum_{j=1}^{N}(q-Z_1)_i^2\right)^{1/2},$$
$$Z_3 = \frac{1}{Z_2^3}\frac{1}{N}\sum_{j=1}^{N}q_j^3, \quad Z_4 = \frac{1}{Z_2^4}\frac{1}{N}\sum_{j=1}^{N}q_j^4, \quad (8)$$

where $N = mn$ is the number of pixels of the CCD-camera.

These parameters characterise the average (Z_1), dispersion (Z_2), asymmetry (Z_3) and kurtosis (Z_4) of the distributions $q(m,n)$.

4. Analysis and discussion of the experimental data

Figure 2 shows a series of Mueller-matrix images M_{ik} of histological sections of tumour biopsies of two types.

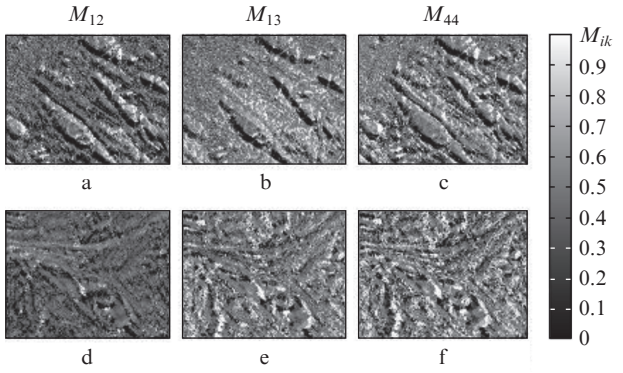

Figure 2. Coordinate distributions ($m \times n$) of the matrix elements (a, d) M_{12}, (b, e) M_{13} and (c, f) M_{44} of the histological sections of (a–c) benign and (d–f) malignant tumours of the uterine wall.

The analysis of the data reveals a common property of Mueller matrices for the samples of both types, i.e., the non-zero difference of the elements $M_{12,13,44}$. This fact confirms the influence of all [relations (1)–(3)] optical anisotropy mechanisms of the myosin and collagen fibril network considered in the modelling analysis. In what follows, we have conducted a comparative statistical [relation (8)] analysis of the maps of the linear birefringence $\delta(m,n)$ (Fig. 3) and linear dichroism $\Delta\tau(m,n)$ (Fig. 4) of the histological sections of fibroids and adenocarcinoma.

The comparative analysis of the data has made it possible to find the following.

Ranges of variation of the coordinate distributions (Fig. 3a, d) of the phase shifts $\delta(m,n)$, found for the samples of both types, are comparable (Figs 3b, e). This can be attributed to the proximity of the birefringence values and transverse dimensions of the fibroid and adenocarcinoma fibrils. Positions of the extrema and the half-width of the histogram $N(\delta)$ are also quite similar (Figs 3c, f). However, the distributions $N(\delta)$ of the adenocarcinoma sample are more asymmetrical. Quantitatively, this is illustrated by the statistical moments found for the histological sections of benign [$Z_1(\delta) = 0.43\pm0.08$, $Z_2(\delta) = 0.16\pm0.03$, $Z_3(\delta) = 0.25\pm0.05$, $Z_4(\delta) = 0.16\pm0.06$] and malignant [$Z_1(\delta) = 0.41\pm0.07$, $Z_2(\delta) = 0.13\pm0.02$, $Z_3(\delta) = 0.38\pm0.06$, $Z_4(\delta) = 0.29\pm0.05$] tumours. This result may be physically attributed to the destruction of the fibrillar network of malignant tumour and to a corresponding decrease in birefringence δ. As a result, the asymmetry Z_3 increases by 1.5 times and the sharpness of the peak Z_4 of the corresponding histogram $N(\delta)$ – by 1.8 times.

Thus, we have found that the sensitivity (higher-order statistical moments $Z_{3,4}$) of the Mueller-matrix method of phase reconstruction [relation (4)] makes it possible to differentiate benign and malignant tumours of the uterine wall.

The analysis of linear dichroism of the histological sections of malignancies shows that it decreases. This property

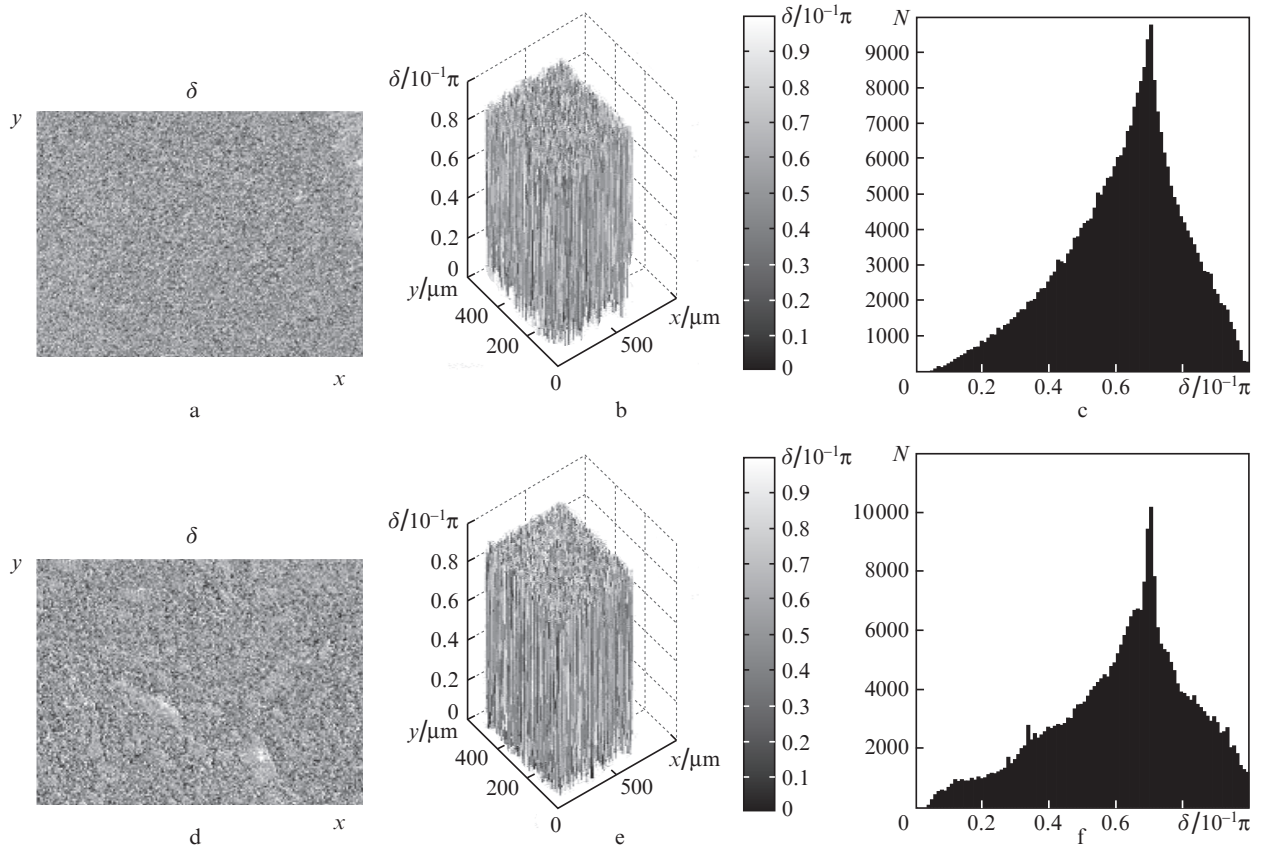

Figure 3. Coordinate (a, d) 2D, (b, e) 3D and (c, f) probability distributions of the phase shifts δ introduced by the histological sections of (a–c) benign and (d–f) malignant tumours of the uterine wall.

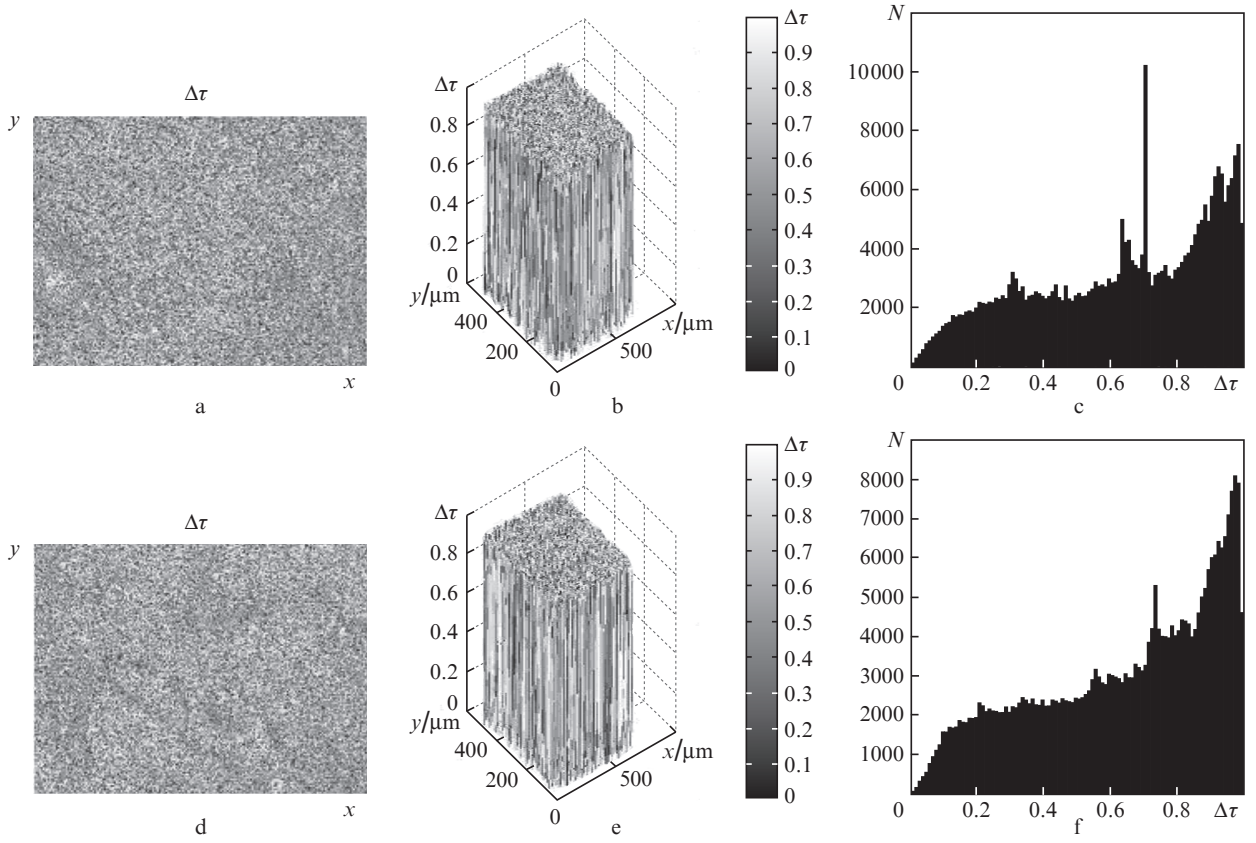

Figure 4. Coordinate (a, d) 2D, (b, e) 3D and (c, f) probability distributions of the linear dichroism $\Delta\tau$ of the histological sections of (a–c) benign and (d–f) malignant tumours of the uterine wall.

manifests itself in the shift of the main extremum of the asymmetric histograms with a sharp peak toward higher values of $\Delta\tau$ (Figs 4c, f). This effect can also be attributed to the morphological process of destruction of fibrillar networks in the diseased tissue of the uterine wall. This transformation of the ordered network (fibroids) to a randomly oriented one (adenocarcinoma) in the ρ directions [relations (1), (2)] leads to closer values of τ_x, τ_y, or $\Delta\tau \to 1$.

The statistical analysis of the coordinate distributions (Figs 4a, d), $\Delta\tau(m,n)$, shows more significant differences between the values $Z_{1,2,3,4}$. We have obtained the following data for the histological sections of benign [$Z_1(\Delta\tau) = 0.69\pm0.03$, $Z_2(\Delta\tau) = 0.38\pm0.04$, $Z_3(\Delta\tau) = 2.04\pm0.18$, $Z_4(\Delta\tau) = 0.59\pm0.13$] and malignant [$Z_1(\Delta\tau) = 0.76\pm0.08$, $Z_2(\Delta\tau) = 0.21\pm0.04$, $Z_3(\Delta\tau) = 0.54\pm0.07$, $Z_4(\Delta\tau) = 1.79\pm0.29$] tumours. One can see that for the adenocarcinoma sample the change in the probability distribution $N(\Delta\tau)$ (Fig. 4f) is accompanied by a decrease in the statistical moments of the second (Z_2) and third (Z_3) orders by 1.8 and 3.8 times, respectively. The statistical moment of the fourth order (Z_4) increases by 3 times. This fact indicates a higher sensitivity of Mueller-matrix method of the optical dichroism parameter reconstruction $\Delta\tau$ [equation (5)] to the type of pathology of the uterine wall.

For the possible clinical use of this method we have performed, within the two statistically significant groups (confidence interval $p < 0.001$) of fibroid (group 1, 32 samples) and adenocarcinoma (group 2, 31 samples) samples, a statistical analysis of the coordinate distributions of the parameters δ and $\Delta\tau$ (Table 1). In addition, for each group we have determined the operating characteristics traditional for evidence-based medicine – sensitivity (Se = $[a/(a + b)]\times100\%$), specificity (Sp = $[c/(c + d)]\times100\%$) and accuracy (Ac = (Se + Sp)/2), where a and b are the number of correct and incorrect diagnoses in group 1; and d and c – the same in group 2 (Table 2).

Table 1. Statistical moments of 1st-to-4th orders characterising the distribution of the optical anisotropy parameters of histological sections of fibroids and adenocarcinoma.

Z_i	Fibroid (32 samples)		Adenocarcinoma (31 samples)	
	δ	$\Delta\tau$	δ	$\Delta\tau$
Z_1	0.42±0.07	0.68±0.02	0.39±0.06	0.74±0.09
Z_2	0.15±0.02	0.36±0.03	0.13±0.02	0.23±0.04
Z_3	0.23±0.04	1.97±0.11	0.36±0.05	0.51±0.06
Z_4	0.19±0.03	0.62±0.14	0.27±0.04	1.74±0.27

For the Mueller-matrix method of reconstruction of the linear birefringence δ and dichroism $\Delta\tau$ parameters, we have found the following quantitative criteria (differences between the averaged values of the statistical moments) of the differentiation of benign and malignant tumours: $\Delta Z_3(\delta) \leftrightarrow 1.56$ and $\Delta Z_4(\delta) \leftrightarrow 1.42$; $\Delta Z_2(\Delta\tau) \leftrightarrow 1.56$, $\Delta Z_3(\Delta\tau) \leftrightarrow 3.86$ and $\Delta Z_4(\Delta\tau) \leftrightarrow 2.8$.

Table 2. Operating characteristics of the Mueller-matrix reconstruction method of the optical anisotropy parameters.

Z_i	δ			$\Delta\tau$		
	Se (%)	Sp (%)	Ac (%)	Se (%)	Sp (%)	Ac (%)
Z_2	94	68	81	84	74	79
Z_3	90	76	83	82	74	78
Z_4	92	74	83	84	72	78

Thus, in the problem of differential diagnosis of benign and malignant changes in uterine tissue efficient were the Mueller-matrix reconstruction methods of both linear birefringence (Ac = 81%–83%) and linear dichroism (Ac = 78%–79%).

These results suggest that the level of azimuthally stable Mueller-matrix mapping accuracy is quite high. According to the criteria of evidence-based medicine [23–25], Ac ~ 80% corresponds to a good quality of a diagnostic test. Note that the most accurate (the gold standard) in the differentiation of benign and malignant tumours are still histological methods. The main drawbacks of traditional methods are large time costs and subjectivity of the final evaluation. Our method is objective and sufficiently fast: the time for a complete diagnostic cycle does not exceed 15 minutes. In addition, in contrast to the data obtained using azimuthally dependent methods, the results of polarisation mapping [13–22] are valid, accurate and quite reproducible.

5. Conclusions

1. Based on the model of the generalised optical anisotropy, which is exhibited by protein networks of biological tissues, we have developed a method of Mueller-matrix reconstruction of the linear birefringence and linear dichroism parameters.

2. We have established a relationship between a set of statistical moments of the 1st-to-4th orders, which characterise the distribution of the phase shifts and linear dichroism coefficient of tissues of the uterus, and pathologies in these tissues.

3. We have demonstrated the diagnostic efficiency of the Mueller-matrix reconstruction method in the differentiation of benign and malignant tumours of the uterine wall.

References

1. Smith M.H., Burke P., Lompado A., Tanner E., Hillman L.W. *Proc. SPIE Int. Soc. Opt. Eng.*, **3991**, 210 (2000).
2. Smith M.H. *Proc. SPIE Int. Soc. Opt. Eng.*, **4257**, 82 (2001).
3. Ushenko Yu.A. *Ukr. J. Phys. Opt.*, **6**, 63 (2005).
4. Tower T.T. *Biophys. J.*, **81**, 2954 (2001).
5. Bueno J.M., Jaronski J. *Ophthal. Physiol. Opt.*, **21**, 384 (2001).
6. Bueno J.M., Vargas-Martin F. *Appl. Opt.*, **41**, 116 (2002).
7. Bueno J.M., Campbell M.C.W. *Ophthal. Physiol. Opt.*, **23**, 109 (2003).
8. Tower T.T., Tranquillo R.T. *Biophys. J.*, **81**, 2964 (2001).
9. Shribak M., Oldenbourg R. *Appl. Opt.*, **42**, 3009 (2003).
10. Petrov V.V., Kryuchyn A.A., Savenkov S.N., Gorbov I.V., Klimov A.S., Oberemok Ye.A. *Data Rec. Storage Proc.*, **12**, 3 (2010).
11. Ushenko Yu.A., Sidor M.I., Bodnar G.B., Koval' G.D. *Kvantovaya Elektron.*, **44**, 785 (2014) [*Quantum Electron.*, **44**, 785 (2014)].
12. Lu S., Chipman R.A. *J. Opt. Soc. Am. A*, **13**, 1106 (1996).
13. Angelsky O.V., Ushenko A.G., Ushenko Yu.A., Pishak V.P., Peresunko A.P., in: *Handbook of Photonics for Biomedical Science.* Ed. by V.V.Tuchin (Boca Raton, London, New York: CRC Press, 2010) p. 283.
14. Ushenko Yu.A., Tomka Yu.Ya., Dubolazov A.V. *Opt. Spektrosk.*, **110**, 814 (2011).
15. Angelsky O.V., Ushenko A.G., Burkovets D.N., Ushenko Yu.A. *Opt. Appl.*, **32**, 591 (2002).
16. Ushenko Y.A. *J. Biomed. Opt.*, **16**, 066006 (2011).
17. Ushenko Y.A., Misevich I.Z., Telenga O.Y., Tomka Y.Y., Karachevtsev A.O. *Opt. Memory Neural Networks (Inform. Opt.)*, **20**, 59 (2011).
18. Ushenko Y.O., Tomka Y.Y., Misevitch I.Z., Istratyy V.V., Telenga O.I. *Opt. Eng.*, **50**, 039001 (2011).
19. Angelsky O.V., Ushenko A.G., Burkovets D.N., Ushenko Yu.A., Jozwicki R., Patorski K. *Opt. Appl.*, **32** (4), 603 (2002).
20. Ushenko Yu.A., Tomka Yu.Ya., Dubolazov A.V., Telen'ga O.Yu. *Kvantovaya Elektron.*, **41**, 273 (2011) [*Quantum Electron.*, **41**, 273 (2011)].
21. Ushenko Y.A. *Optoelectron. Rev.*, **19**, 425 (2011).
22. Ushenko Y.A. *Optoelectron. Rev.*, **19**, 333 (2011).
23. Cassidy L.D. *J. Surg. Res.*, **128**, 199 (2005).
24. Davis C.S. *Statistical Methods of the Analysis of Repeated Measurements* (New York: Springer-Verlag, 2002).
25. Petrie A., Sabin B. *Medical Statistics at a Glance* (Oxford: Blackwell Publ., 2005).